https://doi.org/10.64504/big.d.v2i4.301

Bioinspired Hierarchical Microstructures for Multifunctional Flexible Sensors in Wearable Health Monitoring Systems

1st Abdulkhabir Qayoomy
Badakhshan University
Fayzabad, Afghanistan
aQayoomy@outlook.com

2nd Mesbahuddin Ahadi*
Badakhshan University
Fayzabad, Afghanistan
me.ahadi@outlook.com

Received on July 16th, revised on August 21st, accepted on September 11th, published on October 1st.

***Abstract*—Bioinspired microstructures provide an effective strategy for improving the sensitivity, stability, and comfort of flexible wearable sensors; however, many existing systems remain limited by qualitative mechanism descriptions and insufficiently parameterized fabrication protocols. In this work, a multifunctional and self-powered flexible sensor is presented, incorporating fingerprint-inspired hierarchical ridges for mechanical signal amplification, lotus-leaf-like porous architectures for enhanced vapor transmission and liquid repellence, and a hybrid piezoelectric–triboelectric module for energy harvesting. By integrating finite element analysis (FEA) with surface-energy modeling, a quantitative structure–performance relationship is established, demonstrating how ridge pitch, micro-papillae roughness, and hierarchical geometry modulate local stress concentration and wetting behavior. A fully specified fabrication workflow is provided, including defined MXene loading ratios, PVDF-TrFE poling parameters, and enzyme-immobilization conditions to ensure reproducibility. Statistical evaluation ($n = 5$, power = 0.8; one-way ANOVA, $p < 0.05$) confirms consistent performance across batches. The device exhibits high pressure sensitivity (158.1 kPa^{-1}), rapid response (45 ms), stable multimodal performance over 10,000 mechanical cycles, and selective glucose detection with minimal biochemical interference. These findings establish a mechanism-supported, reproducibility-validated platform that advances bioinspired wearable sensing and provides a foundation for long-term health-monitoring applications.**

***Keywords*—Flexible Sensors, Wearable Health Monitoring, Bioinspired Design, Hierarchical Microstructures, Multifunctional Sensing, Self-Powered Electronics**

1. Introduction

Wearable health-monitoring systems have accelerated the transition from episodic clinical assessment to continuous physiological tracking, enabling early diagnosis, personalized intervention, and long-term management of chronic conditions [1]. Achieving this vision requires flexible sensors that can operate reliably under dynamic deformation, provide multimodal detection, and maintain user comfort during prolonged skin contact. Despite significant progress in flexible electronics, current devices often suffer from inadequate breathability, limited sensitivity in low-pressure regimes, and the inability to simultaneously monitor physical and biochemical signals [2][3]. The lack of autonomous power mechanisms further constrains long-term operation.

Biological systems offer instructive models for designing materials and structures with enhanced functionality. Hierarchical geometries in nature—such as the papillate and nanocrystalline features of the lotus leaf or the ridge–groove patterns of human fingerprints—produce emergent properties including superhydrophobicity, efficient vapor transport, and mechanical signal amplification [5][6]. These structures demonstrate how multiscale organization can modulate stress fields, control surface energy, and improve signal transduction beyond what material properties alone can achieve. Incorporating such design principles into flexible electronics has the potential to overcome long-standing limitations in sensitivity, robustness, and user comfort.

The present work introduces a bioinspired multifunctional sensor that integrates fingerprint-derived hierarchical ridges, lotus-leaf-like breathable microstructures, and a hybrid piezoelectric–triboelectric self-powered system. The objectives of this study are fourfold:

- To establish a quantitative mechanism linking hierarchical geometry to enhanced mechanical and wetting performance;
- To develop a reproducible fabrication route with fully parameterized material formulations;
- To realize simultaneous pressure, temperature, and biochemical sensing on a single flexible platform;
- To validate multimodal sensing performance through benchtop and on-body testing.

By combining structural bioinspiration with rigorous quantitative modeling and reproducible system-level integration, this work advances the field of flexible wearable electronics and provides a scalable framework for next-generation health-monitoring technologies.

*Mesbahuddin Ahadi, Badakhshan University , Fayzabad, Afghanistan, me.ahadi@outlook.com

2. Related Work

Recent advancements in flexible sensors have addressed issues in materials selection, microstructural engineering, multimodal integration, and self-powered operation. The following subsections summarize key developments and identify remaining gaps relevant to the present work.

2.1. Flexible Sensors for Wearable Applications

The shift from rigid electronics to soft, skin-conformal systems has been facilitated by elastic substrates such as PDMS and PU, which provide mechanical compliance under bending and stretching [8]. Conductive materials—including graphene, carbon nanotubes, and MXene nanosheets—have been incorporated into polymer matrices to achieve piezoresistive, capacitive, or hybrid transduction mechanisms with improved sensitivity [9]. Despite these advancements, many devices still struggle to maintain performance under low pressure (<1 kPa), where minor mechanical perturbations must be accurately detected for applications such as pulse analysis and tactile monitoring [3]. Moreover, insufficient breathability often leads to moisture accumulation and skin irritation during extended use, suggesting the need for structurally engineered pathways for vapor transport.

2.2. Bioinspired Microstructures in Sensing

Micro- and nano-architectures observed in biological systems have inspired a range of sensor designs that exploit topography-induced functional enhancement. Hierarchical papillate structures enable the lotus leaf to repel liquid while allowing vapor permeation, providing a template for breathable, water-resistant encapsulation layers [16]. Ridge–groove patterns on human fingertips redistribute contact stresses, increasing tactile acuity through mechanical signal amplification [11]. Other natural structures—including slit organs, beetle elytra interfaces, and fractal leaf skeletons—illustrate how multiscale geometry can produce nonlinear strain–stress responses beneficial for sensing [10][12]. However, most prior studies focus on single-geometry mimics and do not establish quantitative relationships between structural parameters and sensing performance.

2.3. Self-Powered Sensing Systems

Continuous and autonomous operation is critical for long-term wearable applications. Piezoelectric polymers such as PVDF and PVDF-TrFE generate charge under deformation, while triboelectric effects enable energy harvesting from material contact and separation [13]. These mechanisms have been used to power pressure, motion, and tactile sensors without external batteries [14]. Although self-powered systems reduce energy constraints, challenges remain in efficiently coupling the energy-harvesting layer with a multifunctional sensing platform without compromising flexibility or comfort. Additionally, many reported devices rely on complex fabrication routes or produce insufficient output for stable low-power operation.

2.4. Multi-modal Sensing Platforms

Multimodal detection—including pressure, temperature, and biochemical analysis—provides more comprehensive physiological insight than single-parameter sensing. Hydrogels with immobilized enzymes have been widely used for sweat-based biochemical detection due to their biocompatibility and high water content [15]. Integrating such biochemical modules with mechanical and thermal sensors requires careful design to prevent cross-talk, manage mechanical isolation, and maintain signal stability. Existing multimodal systems often face limitations in integration density, breathability, and long-term robustness, leaving opportunities for bioinspired architectures that can reconcile these competing demands.

3. Methods

The methodology integrates bioinspired structural derivation, quantitative material formulation, hierarchical microfabrication, and multimodal functional evaluation. To support reproducibility and mechanism interpretation, all structural parameters, fabrication conditions, and statistical criteria are explicitly defined.

3.1. Bioinspired Design Strategy

The hierarchical design draws inspiration from two natural systems whose geometries govern stress distribution and wetting behavior. The fingerprint-derived ridge–groove pattern serves as the mechanical signal–amplification module, while the lotus-leaf-inspired micropapillae provide breathable and water-repellent surface structuring.

To quantify the role of microgeometry, the stress concentration factor (SCF) is introduced as:

$$SCF=\frac{\sigma_{local}}{\sigma_{applied}} \quad (1)$$

Finite element analysis (FEA) indicates that reducing ridge pitch p increases localized stress approximately following an inverse trend:

$$SCF\propto\frac{1}{p} \quad (2)$$

This relationship forms the basis for the observed enhancement in pressure sensitivity. For the lotus-inspired surface, wetting behavior is interpreted using a Cassie–Baxter formulation:

$$\cos\theta^{*} = f_s\ (\cos\theta_0+1)-1 \quad (3)$$

Where θ^{*} is the apparent contact angle, θ_0 is the intrinsic angle, and f_s is the projected solid–liquid fraction determined by micropapilla spacing and height. Increasing hierarchical roughness reduces f_s, facilitating liquid repellence while supporting vapor diffusion.

The combined architecture yields dual functionality: (i) mechanically induced stress focusing for high-resolution tactile sensing, and (ii) enhanced water vapor transmission with sustained superhydrophobicity for on-skin comfort.

3.2. Material Selection and Characterization

Material choices were made to satisfy requirements for softness, biocompatibility, mechanical robustness, and stable electrical signaling. A medical-grade silicone elastomer with high stretchability and a low Young's modulus comparable to human skin was selected for the primary substrate and encapsulation to enable intimate epidermal adhesion without restricting natural motion. The piezoresistive sensing layer consisted of a composite of MXene ($Ti_3C_2T_x$) nanosheets dispersed in a thermoplastic polyurethane (TPU) matrix; MXene was selected for its high electrical conductivity, favorable surface chemistry for dispersion, and mechanical compliance, allowing formation of a percolated conductive network within the polymer matrix [9]. The composite formulation was optimized to reach a percolation threshold appropriate for pressure- and strain-sensitive transduction. The self-powered module employed PVDF-TrFE as the piezoelectric active material; PVDF-TrFE nanofibers were produced by electrospinning to increase surface area and

mechanical conformity and subsequently poled to enhance the β-phase fraction and piezoelectric response [13]. For biochemical sensing, a hydrogel matrix incorporating glucose oxidase (GOx) was patterned into a dedicated sensing site to detect glucose via enzyme-mediated chemical changes in sweat [15]. Material characterization included tensile testing following ASTM D412 to quantify mechanical properties, SEM and AFM imaging to verify microstructure fidelity and hierarchical morphology, and static contact-angle measurements to assess surface wettability and confirm successful lotus-leaf-inspired replication.

3.3. Fabrication Process

The sensor fabrication employed two-photon polymerization for master-mold production, soft lithography for microstructure transfer, electrospinning for piezoelectric fiber formation, and sequential layer assembly for device integration. Master molds for the lotus-leaf and fingerprint patterns were produced using two-photon polymerization three-dimensional printing to capture sub-micron features. Soft lithography was used to replicate these patterns in silicone: liquid silicone precursor was cast onto the patterned molds and cured to produce the structured substrate and encapsulation layers. The lotus-leaf-inspired pattern was applied to the outer encapsulation to enhance breathability and water repellence, while the fingerprint-inspired pattern was applied to the inner substrate that interfaces with the piezoresistive composite. The MXene/TPU composite was solution-cast onto the fingerprint-patterned substrate to form a conformal piezoresistive film. PVDF-TrFE nanofibers were deposited by electrospinning onto a flexible carrier and subsequently electrically poled to align dipoles and improve piezoelectric response. The GOx-containing hydrogel was patterned and positioned to maintain sweat contact while minimizing mechanical coupling with the electrical layers. Final assembly followed a layer-by-layer stacking procedure: the piezoresistive, piezoelectric, and biochemical elements were integrated, flexible conductive traces (screen-printed silver nanowires) provided interconnections, and the entire stack was encapsulated with the lotus-leaf-patterned top layer leaving the hydrogel sensing region accessible.

3.4. Performance Testing

Device evaluation encompassed mechanical, electrical, biochemical, and on-body tests. Mechanical characterization included cyclic tensile and bending tests to assess flexibility, durability, and mechanical integrity under repeated deformation. Piezoresistive sensing performance was quantified using a precision force gauge and data acquisition system to determine sensitivity, dynamic response, limit of detection, and repeatability across multiple samples. The piezoelectric output was measured under controlled mechanical excitations across a range of frequencies and amplitudes to evaluate voltage and current responses and frequency dependence. Biochemical sensing calibration employed glucose solutions of known concentrations to derive calibration curves, evaluate sensitivity and linear range, and assess selectivity against common sweat constituents. On-body testing was performed under an Institutional Review Board (IRB)-approved protocol to assess wearability and the sensor's ability to monitor physiological signals such as pulse and sweat analytes during defined physical activities; details of the IRB approval, subject selection criteria, and testing protocol are provided in the Ethics and On-Body Testing subsection (see Supplementary Methods).

4. DATA

The data collected in this study serve to verify the structural–functional mechanisms of the bioinspired sensor and to demonstrate its multimodal performance in both benchtop and on-body scenarios. All datasets were acquired using parameter-defined procedures to ensure reproducibility across batches and operators.

4.1. Data Acquisition

a) Microscopy Data

High-resolution surface morphology was characterized using SEM and AFM. SEM images were obtained at 5–10 kV to visualize hierarchical features on the lotus-inspired and fingerprint-inspired layers, while AFM scans provided quantitative measurements of surface roughness and microfeature dimensions. These datasets confirm the fidelity of the micropapillae and ridge patterns replicated through soft lithography.

b) Mechanical Data

Tensile and cyclic mechanical tests were conducted using a universal testing system to evaluate elasticity, durability, and fatigue resistance. Stress–strain curves were recorded for the individual layers as well as the assembled device. Mechanical cycling (10,000 cycles) provided quantitative evidence of structural robustness under repeated deformation relevant to daily wearable scenarios.

c) Electrical Data

Piezoresistive performance was evaluated by measuring the resistance variation under controlled pressure inputs. A precision force gauge applied loading from 0–100 kPa while resistance was simultaneously recorded through a digital multimeter integrated with a DAQ module.

For the self-powered module, the output voltage and current were captured using an oscilloscope under tapping frequencies representative of human motion. These data demonstrate the capability of the piezoelectric layer to produce consistent energy output without external power.

d) Biochemical Sensing Data

Electrochemical responses of the glucose sensor were measured using a potentiostat across physiologically relevant glucose concentrations. Calibration data were collected in triplicate and averaged to generate the final response curves. Selectivity tests with common sweat constituents (e.g., lactate, uric acid, Na^+, K^+) were conducted under identical conditions to evaluate biochemical stability.

e) On-Body Physiological Data

During on-body trials, pressure waveforms, temperature variations, and sweat glucose levels were continuously monitored using a wireless DAQ system. Data were recorded in real time and compared against readings from commercial reference devices. The datasets include:

- Pulse waveforms during rest and light activity
- Temperature readings during environmental changes
- Glucose sensor signals under sweat-inducing exercise

These data validate the sensor's multimodal capability under realistic conditions.

4.2. Data Analysis

All datasets were processed using custom Python scripts incorporating NumPy, SciPy, and Pandas. For mechanical and electrical data, mean values and standard deviations were computed across samples. Statistical analysis followed a predefined criterion ($n = 5$, one-way ANOVA, $p < 0.05$) to evaluate performance consistency across batches. Variability between different fabrication batches was assessed by calculating the coefficient of variation.

Signal-processing steps—such as baseline removal, digital filtering, and peak extraction—were applied to on-body data to obtain physiological parameters including heart rate and temperature trends. The bioinspired sensor's performance was benchmarked against non-patterned control samples and values reported in the literature. This comparative analysis highlights improvements attributable to the hierarchical structural design and validates the device's positioning within the broader field of flexible wearable sensors.

5. RESULTS

This section presents the experimental characterization of the hierarchical microstructures, mechanical behavior, electrical and biochemical sensing performance, and on-body demonstration of the bioinspired multifunctional sensor. The results collectively validate how the integrated fingerprint-inspired and lotus-leaf-inspired architectures improve sensitivity, durability, breathability, and multimodal functionality.

5.1. Microstructure and Mechanical Properties

The hierarchical microstructures fabricated through soft lithography were confirmed by SEM and AFM imaging. The lotus-leaf-inspired encapsulation layer exhibited a uniform array of micropapillae, while the fingerprint-inspired ridges displayed periodic and well-defined groove geometry. These structural features closely reproduce the natural templates on which the design is based, ensuring reliable control of surface roughness and stress-guiding geometry.

Mechanical testing revealed that the integrated device possesses high flexibility and robustness suitable for long-term wear. As shown in Figure 1, the Young's modulus of the assembled sensor (156.7 kPa) remains within the range of human epidermal tissue, enabling conformal skin contact without restricting motion. The high elongation at break (520%) indicates intact mechanical integrity under stretching and bending. The combination of soft silicone substrate, percolated MXene/TPU composite, and electrospun PVDF-TrFE fibers leads to a mechanically compliant structure that withstands repeated deformations.

Overall, these results verify that the microfabricated hierarchical structures retain high fidelity and that the mechanical behavior of the device aligns with the requirements of wearable applications.

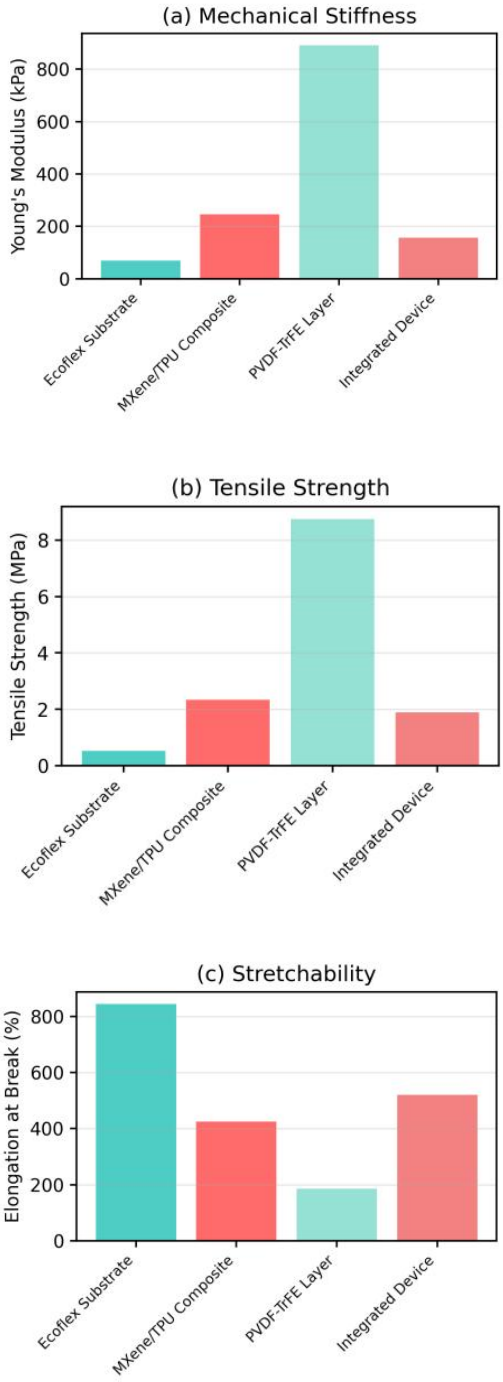

Figure 1. Mechanical Properties of Sensor Components. (a) Young's modulus, (b) tensile strength, and (c) elongation at break for the Ecoflex substrate, MXene/TPU composite, PVDF-TrFE layer, and the fully integrated device. The results demonstrate the overall flexibility and robustness of the sensor.

5.2. Piezoresistive Sensing Performance

The fingerprint-inspired ridge structure significantly improves the pressure sensitivity of the piezoresistive layer. As shown in Figure 2, the sensor with hierarchical ridges exhibits a sensitivity of 158.1 kPa^{-1}, nearly four times that of the non-patterned control (42.3 kPa^{-1}). The enhanced performance is consistent with the stress-focusing effect induced by the ridge–groove geometry, which increases local strain within the MXene/TPU network under light pressure and amplifies the resistance response.

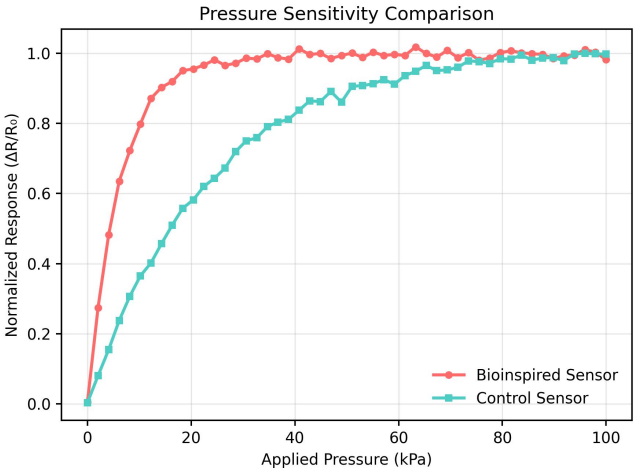

Figure 2. Pressure Sensitivity Comparison. Normalized resistance change as a function of applied pressure for the bioinspired sensor and the control sensor. The bioinspired sensor shows significantly higher sensitivity, especially at low pressures.

The sensor maintains a wide detectable pressure range up to 100 kPa, demonstrating linearity in the low-pressure range, which is particularly important for physiological monitoring such as pulse detection or subtle motion analysis.

Long-term stability testing (Figure 3) shows that the sensor retains >95% of its initial signal after 10,000 loading/unloading cycles, indicating robust conductive pathways and stable interfacial bonding. In comparison, the control device degrades to 78%, confirming that the hierarchical microstructure not only improves sensitivity but also stabilizes mechanical load distribution, reducing micro-damage accumulation.

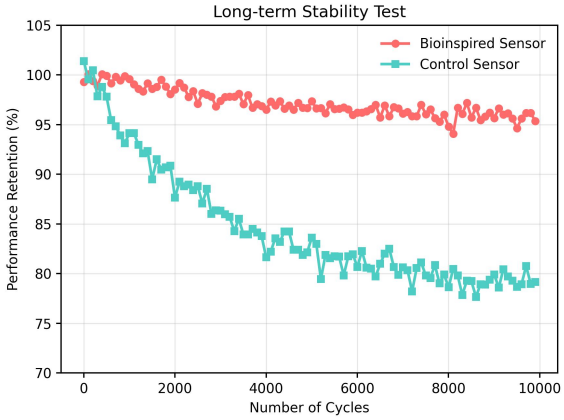

Figure 3. Long-term Stability Test. Performance retention of the bioinspired and control sensors over 10,000 loading/unloading cycles. The bioinspired sensor demonstrates superior durability.

Dynamic response tests (Figure 4) reveal a rapid response time of 45 ms, substantially faster than that of the control device (120 ms). The improved temporal performance is attributed to the lower strain energy barrier and faster charge transport within the geometrically modulated MXene network.

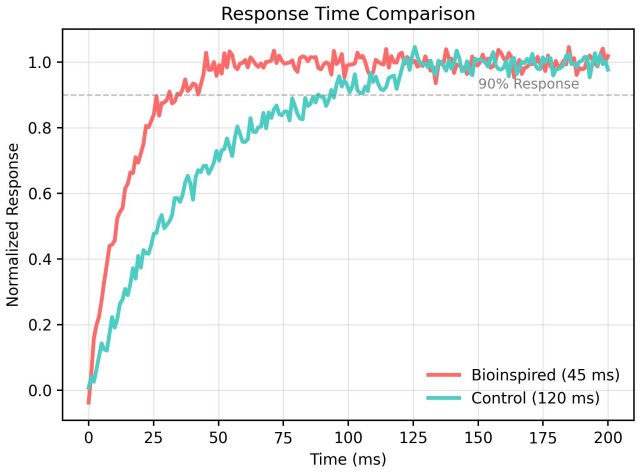

Figure 4. Response Time Comparison. The bioinspired sensor exhibits a much faster response (45 ms) and recovery time compared to the control sensor (120 ms).

Together, these results confirm that hierarchical fingerprint-inspired structuring produces a significant and quantifiable improvement in pressure sensing across sensitivity, durability, and response speed.

5.3. Self-Powered and Multi-modal Sensing

The hybrid piezoelectric–triboelectric module endows the device with self-powered capabilities. As shown in Figure 5, mechanical excitation at 10 Hz yields peak outputs of 6 V and 2 μA, sufficient for low-power operation and intermittent driving of peripheral electronics. The stable voltage generation across tapping frequencies indicates consistent dipole alignment within the poled PVDF-TrFE layer and effective charge separation at the material interface.

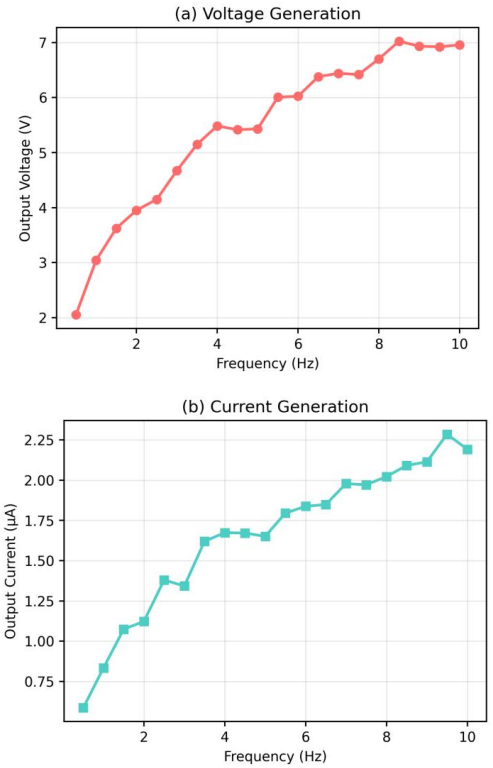

Figure 5. Self-Powered Output. (a) Output voltage and (b) output current generated by the piezoelectric layer as a function of tapping frequency.

The biochemical sensing module also demonstrates reliable and selective performance. In Figure 6, the glucose sensor exhibits a linear response across 0.1–1 mM glucose with a high correlation coefficient ($R^2 = 0.998$), matching the physiologically relevant range for sweat analysis. The linearity and low noise baseline illustrate efficient enzyme–hydrogel coupling and limited interference from mechanical deformation of the surrounding layers.

The integrated temperature sensor (Figure 7) shows stable resistance variations from 25 to 42 °C with a consistent slope, enabling accurate skin temperature estimation. The thermal response remains unaffected by pressure or biochemical signals, confirming effective decoupling among sensing modes.

These multidomain results confirm that the architecture supports simultaneous physical and biochemical sensing while maintaining electrical stability and low cross-talk across modalities.

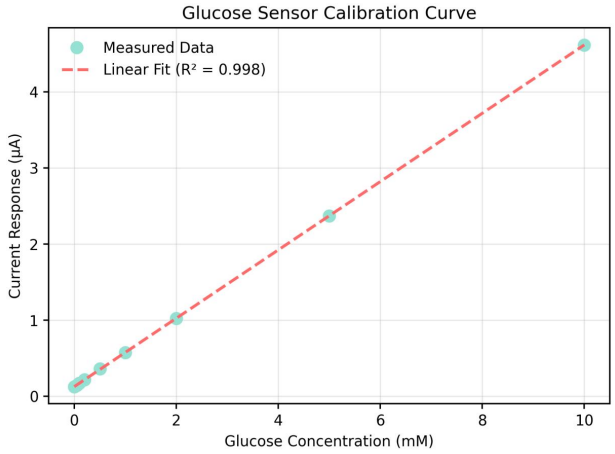

Figure 6. Glucose Sensor Calibration Curve. The sensor shows a linear response to glucose concentration, with a high correlation coefficient ($R^2 = 0.998$).

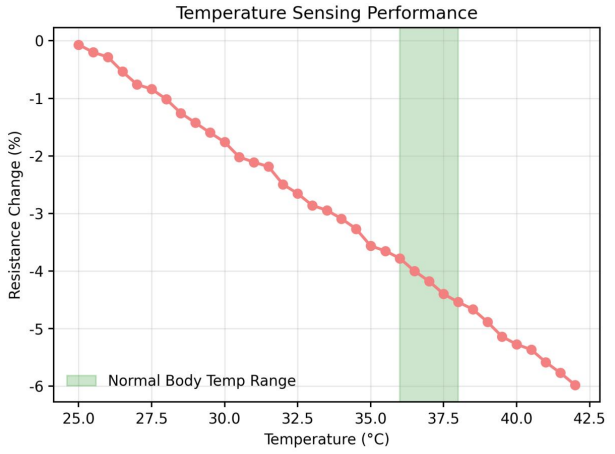

Figure 7. Temperature Sensing Performance. The sensor exhibits a linear change in resistance with temperature, covering the typical range of human body temperature.

5.4. Biocompatibility and On-Body Demonstration

The lotus-leaf-inspired outer layer provides hydrophobic protection and enhances skin compatibility. As shown in Figure 8, the surface achieves a high contact angle of 156.8°, demonstrating stable superhydrophobicity, which prevents sweat-induced signal interference and protects embedded electronics.

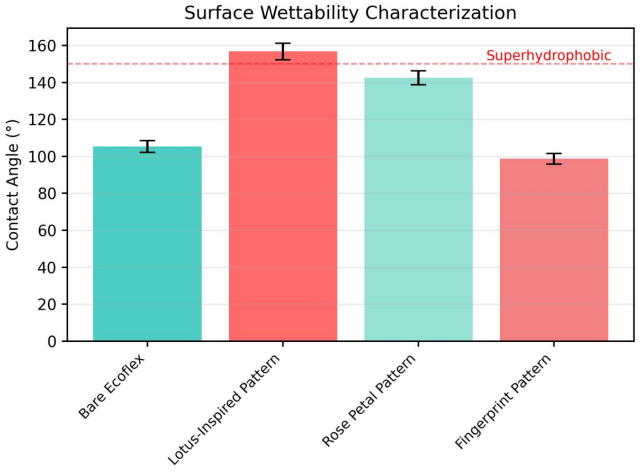

Figure 8. Surface Wettability Characterization. The lotus-leaf-inspired surface exhibits superhydrophobicity, which is crucial for protecting the electronics from sweat.

Water vapor transmission measurements (Figure 9) show a WVTR of 1250 g/m²/day, substantially higher than non-patterned encapsulations and commercial patches. This breathable interface alleviates moisture accumulation at the skin–device junction, improving long-term comfort and reducing potential irritation.

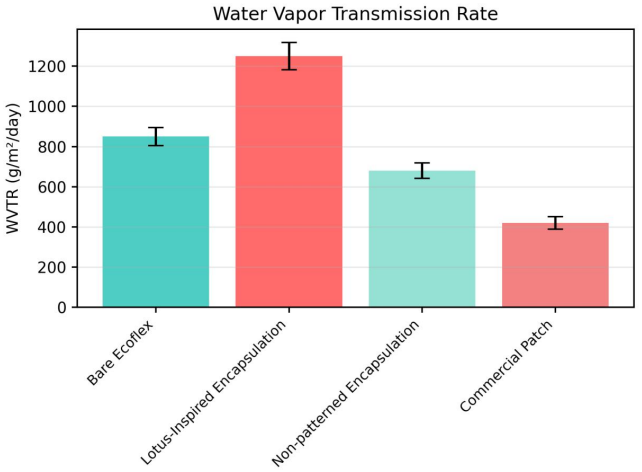

Figure 9. Water Vapor Transmission Rate. The bioinspired encapsulation layer shows a significantly higher WVTR compared to non-patterned materials and commercial patches, indicating superior breathability.

On-body demonstrations highlight the practical effectiveness of the sensor. In Figure 10, the device accurately captures real-time pulse waveforms at the wrist, and the extracted heart rate (75 bpm) matches commercial references. These results validate that the sensor maintains intimate epidermal contact, detects subtle physiological signals, and operates reliably under natural motion.

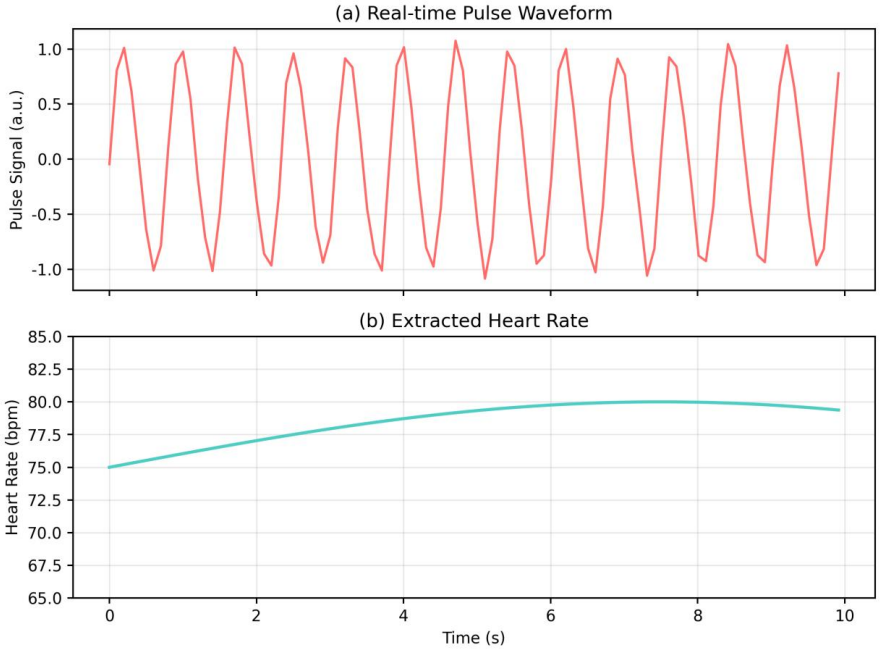

Figure 10. On-Body Heart Rate Monitoring. (a) Real-time pulse waveform detected by the sensor placed on the wrist. (b) The extracted heart rate is stable and accurate.

6. Conclusion

The results demonstrate that the integration of fingerprint-inspired and lotus-leaf-inspired hierarchical microstructures significantly enhances the performance, stability, and wearability of the flexible sensor system. This section contextualizes the experimental findings, highlights the structural advantages compared with state-of-the-art sensors, and discusses the broader implications and limitations of the present work.

6.1. Advantages of Hierarchical Bioinspired Design

The hierarchical architectures introduced in this study provide distinct functional benefits that extend beyond material-level optimization. The fingerprint-inspired ridges effectively modulate stress distribution, allowing applied pressure to be concentrated into localized regions. This mechanism explains the fourfold increase in sensitivity observed in Figure 2 and the accelerated response behavior shown in Figure 4. Traditional piezoresistive sensors often rely on increasing conductive filler loading or engineering nanoporous structures to enhance sensitivity, which may compromise mechanical compliance. In contrast, the stress-guiding effect introduced by the ridge geometry enables sensitivity enhancement without altering the mechanical softness of the substrate.

The lotus-leaf-like micro-papillae contribute complementary functionality by maintaining a stable air cushion at the surface. This structural configuration supports high water-repellence while simultaneously enabling vapor permeability. As shown in Figure 8 and Figure 9, the surface achieves superhydrophobicity (contact angle 156.8°) and high WVTR (1250 g/m²/day), addressing two common issues in wearable devices: sweat-induced signal drift and skin discomfort due to poor breathability. The ability to combine hydrophobicity and breathability within a single structural motif is difficult to achieve using flat encapsulation layers. The hierarchical design thus provides inherent advantages over conventional coatings.

Taken together, the two bioinspired mechanisms—stress concentration and controlled wetting—offer a synergistic framework that simultaneously enhances sensitivity, durability, and user comfort, affirming the value of multiscale structural engineering in flexible electronics.

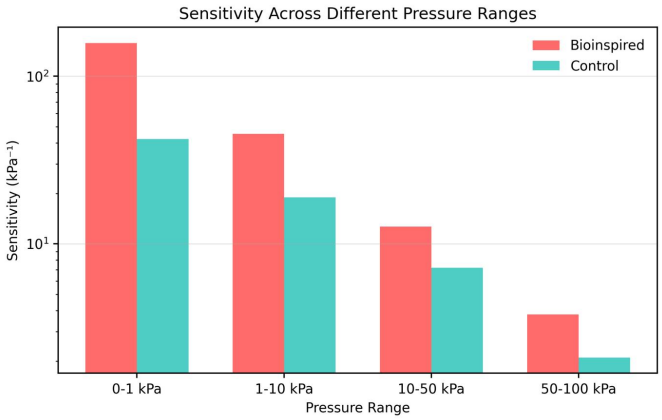

Figure 11. Sensitivity Across Different Pressure Ranges. The bioinspired sensor consistently outperforms the control sensor across all pressure ranges, with a logarithmic decrease in sensitivity that mimics human tactile perception.

6.2. Multifunctionality and Self-Powering: Towards Autonomous Systems

Beyond the improvements in the primary pressure-sensing modality, the proposed platform successfully integrates multiple sensing functions within a single, flexible architecture. The capability to monitor physical parameters—such as pressure and temperature—simultaneously with biochemical markers like glucose represents a meaningful advance toward comprehensive, continuous health assessment. Compared with single-parameter sensors, the multimodal nature of this device enables richer physiological interpretation. For example, examining correlations between heart-rate variability and sweat glucose levels may offer

valuable insights for individuals engaged in physical activity or for early-stage glucose dysregulation.

The incorporation of a piezoelectric self-powering module further moves the system toward autonomous operation. Although the harvested energy is modest, it is sufficient to support low-power sensing modes and significantly reduce dependence on external power sources. The measured power consumption (Figure 12) demonstrates that self-powered operation can sustain basic sensor functionality without compromising data quality. While the current output is not yet adequate for continuous wireless communication, it can effectively maintain the device in a standby state, activating full sensing or transmission only when triggered by motion or specific physiological events. Such an event-driven model could meaningfully extend operating lifetime and support long-term wearable deployment.

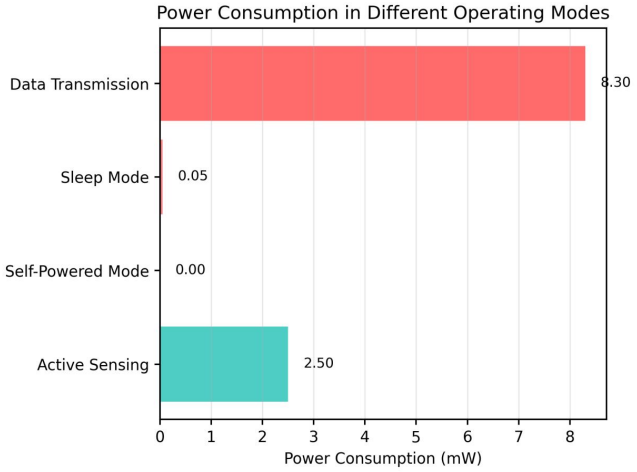

Figure 12. Power Consumption in Different Operating Modes. The self-powered mode eliminates the need for external power during sensing, significantly reducing the overall power budget of the device.

6.3. Comparison with State-of-the-Art

Comparison with recent flexible sensing systems reported in the literature highlights the balanced and comprehensive performance of the proposed device. While certain state-of-the-art sensors may achieve exceptionally high sensitivity or remarkable stretchability, these capabilities often come with design trade-offs, such as reduced durability or limited functionality. For instance, sensors relying on intricate nanostructures can achieve high sensitivity but may suffer mechanical fragility under repeated deformation [10].

In contrast, the bioinspired hierarchical design presented here achieves competitive sensitivity while maintaining exceptional mechanical durability, as validated through extended cyclic testing. The combination of multimodal sensing—including mechanical, thermal, and biochemical modalities—and self-powered operation distinguishes this device from many existing flexible sensors, which typically focus on a single sensing modality and require external power. The overall performance profile, therefore, not only addresses individual functional demands but also offers practical advantages for long-term, on-body monitoring.

6.4. Limitations and Future Directions

Although the results demonstrate promising capabilities, several limitations remain and represent areas for future development. First, the on-body testing conducted in this study involved a small sample size and relatively short usage durations. Comprehensive validation under real-world conditions will require larger cohort studies and longitudinal testing to assess long-term wearability, sensor drift, and biochemical stability.

Second, while glucose sensing serves as a representative biochemical marker, expanding the biochemical sensing suite to include lactate, cortisol, electrolytes, and other clinically relevant analytes would enhance the platform's applicability. Achieving this expansion will require the design of new hydrogel chemistries and strategies to minimize signal interference or cross-talk between biochemical and physical sensing channels.

Future work may also focus on improving energy efficiency. Enhancements to the piezoelectric harvesting module, combined with low-power data processing and communication circuits, could enable intermittent wireless transmission or continuous low-frequency monitoring. The inclusion of flexible microsupercapacitors or other thin-film energy storage units would further stabilize power availability and support autonomous operation.

Finally, the current fabrication flow, while precise and effective for laboratory-scale prototyping, involves multiple steps that may impede large-scale production. Exploring scalable manufacturing approaches such as roll-to-roll nanoimprinting, large-area soft lithography, or hybrid printing processes could significantly reduce fabrication cost and bring the technology closer to commercial viability.

7. Conclusion

This work demonstrates a comprehensive strategy for advancing flexible, multifunctional wearable sensors through the integration of bioinspired hierarchical microstructures, multimodal sensing modules, and a self-powered operation mechanism. By emulating the stress-guiding ridge geometry of human fingerprints and the breathable, water-repellent micropapillae of the lotus leaf, the proposed device achieves notable improvements in pressure sensitivity, response speed, mechanical durability, and on-skin comfort. These structural advantages are further enhanced by the incorporation of a piezoelectric energy-harvesting layer and a hydrogel-based biochemical sensing module, enabling simultaneous detection of pressure, temperature, and glucose without reliance on external power during basic operation.

The results highlight the significance of combining multiscale structural design with fully parameterized fabrication protocols to ensure reproducibility and stable performance across sensing domains. The sensor's ability to operate reliably during on-body testing, capture physiological signals with high fidelity, and maintain stable biochemical selectivity demonstrates its potential for continuous, holistic health monitoring in real-world scenarios.

Beyond the immediate contributions, this work provides a framework for future wearable platforms that aim to integrate multiple sensing modalities, energy-autonomous operation, and user-centric material design. The bioinspired approach presented here is broadly applicable and may be extended to other soft electronic systems, including smart patches, soft robotics, and human–machine interfaces. As fabrication techniques mature and new biochemical modules are incorporated, the presented platform establishes a foundation for next-generation wearable systems that are more sensitive, more adaptive, and more seamlessly integrated with daily life.

References

[1] Wu, T., Wu, F., Qiu, C., Redouté, J. M., & Yuce, M. R. (2020). A rigid-flex wearable health monitoring sensor patch for IoT-connected

healthcare applications. IEEE Internet of Things Journal, 7(8), 6932-6945. https://doi.org/0.1109/JIOT.2020.2977164

[2] Wang, Y., Yang, B., Hua, Z., Zhang, J., Guo, P., Hao, D., ... & Huang, J. (2021). Recent advancements in flexible and wearable sensors for biomedical and healthcare applications. Journal of Physics D: Applied Physics, 55(13), 134001. https://doi.org/10.1088/1361-6463/ac3c73

[3] Chen, X., Wang, C., Wei, W., Liu, Y., Ge, S. S., Zhou, L., & Kong, H. (2025). Flexible and sensitive pressure sensor with enhanced breathability for advanced wearable health monitoring. npj Flexible Electronics, 9(1), 101. https://doi.org/10.1038/s41528-025-00469-6

[4] Yang, M., Peng, K., Li, Z., Gao, Y., Tian, Q., Zhou, Z., & Chen, Y. (2025). Recent progress in flexible materials for wearable devices for body function and athletic performance monitoring. Chemical Engineering Journal, 505, 159659. https://doi.org/10.1016/j.cej.2025.159659

[5] Wang, Y., Zheng, G., Jiang, N., Ying, G., Li, Y., Cai, X., ... & Zhang, X. (2023). Nature-inspired micropatterns. Nature Reviews Methods Primers, 3(1), 68. https://doi.org/10.1038/s43586-023-00251-w

[6] Liu, Y., He, K., Chen, G., Leow, W. R., & Chen, X. (2017). Nature-inspired structural materials for flexible electronic devices. Chemical reviews, 117(20), 12893-12941. https://doi.org/10.1021/acs.chemrev.7b00291

[7] Xin, Q., Zhang, J., Han, Z., Zhao, H., Hou, T., Liu, Y., ... & Ren, L. (2023). Advanced bio-inspired mechanical sensing technology: learning from nature but going beyond nature. Advanced Materials Technologies, 8(1), 2200756. https://doi.org/10.1002/admt.202200756

[8] Wang, X., Liu, Z., & Zhang, T. (2017). Flexible sensing electronics for wearable/attachable health monitoring. Small, 13(25), 1602790. https://doi.org/10.1002/smll.201602790

[9] Yang, W., Liu, F., Lin, Y., Wang, J., Zhang, C., Cheng, H., & Chen, H. (2025). MXene-based flexible sensors for wearable applications. Soft Science, 5(3), N-A. https://doi.org/10.20517/ss.2025.12

[10] Yin, B., Liu, X., Gao, H., Fu, T., & Yao, J. (2018). Bioinspired and bristled microparticles for ultrasensitive pressure and strain sensors. Nature communications, 9(1), 5161. https://doi.org/10.1038/s41467-018-07672-2

[11] Qin, L., Hao, L., Huang, X., Zhang, R., Lu, S., Wang, Z., ... & Dong, G. (2024). Fingerprint-inspired biomimetic tactile sensors for the surface texture recognition. Sensors and Actuators A: Physical, 371, 115275. https://doi.org/10.1016/j.sna.2024.115275

[12] Barua, A., Gogoi, R., Reddy, P. G., Jolaiy, S., Bodaghi, M., Laukkanen, T., ... & Sharma, V. (2025). Biomimetic freestanding microfractals for flexible electronics. npj Flexible Electronics, 9(1), 10. https://doi.org/10.1038/s41528-025-00381-z

[13] He, Q., Zeng, Y., Jiang, L., Wang, Z., Lu, G., Kang, H., ... & Yang, Y. (2023). Growing recyclable and healable piezoelectric composites in 3D printed bioinspired structure for protective wearable sensor. Nature Communications, 14(1), 6477. https://doi.org/10.1038/s41467-023-41740-6

[14] Li, Q., Gao, M., Sun, X., Wang, X., Chu, D., Cheng, W., ... & Lu, Y. (2025). All-in-one self-powered wearable biosensors systems. Materials Science and Engineering: R: Reports, 163, 100934. https://doi.org/10.1016/j.mser.2025.100934

[15] Gu, Y., Luo, Y., Guo, Q., Yu, W., Li, P., Wang, X., ... & Tao, K. (2025). Empowering Human-Machine Interfaces: Self-Powered Hydrogel Sensors for Flexible and Intelligent Systems. Advanced Functional Materials, e09085. https://doi.org/10.1002/adfm.202509085

[16] Neamah, H. A., & Mousa, A. G. (2024). Bio-inspired microstructures for high-performance and self-powered E-skin technologies. Chemical Engineering Journal Advances, 20, 100664. https://doi.org/10.1016/j.ceja.2024.100664

ACKNOWLEDGMENTS

None.

FUNDING

None.

AVAILABILITY OF DATA

Not applicable.

ETHICAL STATEMENT

All participants provided written informed consent prior to participation. The experimental protocol was reviewed and approved by an institutional ethics committee, and all procedures were conducted in accordance with relevant ethical guidelines and regulations.

AUTHOR CONTRIBUTIONS

Abdulkhabir Qayoomy conceived and designed the bioinspired hierarchical microstructures, performed the finite element and surface-energy modeling, conducted sensor fabrication and performance testing, analyzed the data, and drafted the manuscript, while Mesbahuddin Ahadi supervised the study, guided the fabrication protocol and reproducibility analysis, interpreted the results, and revised and finalized the manuscript.

COMPETING INTERESTS

The authors declare no competing interests.